

Uncertainty in high-resolution hydrological projections: Partitioning the influence of climate models and natural climate variability

Jorge Sebastián Moraga¹  | Nadav Peleg^{1,2}  | Peter Molnar¹  |
Simone Fatichi³  | Paolo Burlando¹

¹Institute of Environmental Engineering, ETH Zürich, Zürich, Switzerland

²Institute of Earth Surface Dynamics, University of Lausanne, Lausanne, Switzerland

³Department of Civil and Environmental Engineering, National University of Singapore, Singapore, Singapore

Correspondence

Jorge Sebastián Moraga, Institute of Environmental Engineering, ETH Zürich, Zürich, Switzerland.

Email: moraga@ifu.baug.ethz.ch

Funding information

Bundesamt für Umwelt, Grant/Award Number: 15.0003.PJ/Q123-0588

Abstract

A major challenge in assessing the impacts of climate change on hydrological processes lies in dealing with large degrees of uncertainty in the future climate projections. Part of the uncertainty is owed to the intrinsic randomness of climate phenomena, which is considered irreducible. Additionally, modelling the response of hydrological processes to the changing climate requires the use of a chain of numerical models, each of which contributes some degree of uncertainty to the final outputs. As a result, hydrological projections, despite the progressive increase in the accuracy of the models along the chain, still display high levels of uncertainty, especially at small temporal and spatial scales. In this work, we present a framework to quantify and partition the uncertainty of hydrological processes emerging from climate models and internal variability, across a broad range of scales. Using the example of two mountainous catchments in Switzerland, we produced high-resolution ensembles of climate and hydrological data using a two-dimensional weather generator (AWE-GEN- 2d) and a distributed hydrological model (TOPKAPI-ETH). We quantified the uncertainty in hydrological projections towards the end of the century through the estimation of the values of signal-to-noise ratios (STNR). We found small STNR absolute values (<1) in the projection of annual streamflow for most sub-catchments in both study sites that are dominated by the large natural variability of precipitation (explains ~70% of total uncertainty). Furthermore, we investigated in detail specific hydrological components that are critical in the model chain. For example, snow-melt and liquid precipitation exhibit robust change signals, which translates into high STNR values for streamflow during warm seasons and at higher elevations, together with a larger contribution of climate model uncertainty. In contrast, projections of extreme high flows show low STNR values due to large internal climate variability across all elevations, which limits the potential for narrowing their estimation uncertainty.

KEYWORDS

climate change, hydrological modelling, hydrological uncertainty, uncertainty partition, weather generator

This is an open access article under the terms of the [Creative Commons Attribution-NonCommercial](https://creativecommons.org/licenses/by-nc/4.0/) License, which permits use, distribution and reproduction in any medium, provided the original work is properly cited and is not used for commercial purposes.

© 2022 The Authors. *Hydrological Processes* published by John Wiley & Sons Ltd.

1 | INTRODUCTION

One of the main challenges in climate change impact studies is to quantify the large uncertainties associated with climate projections (Hoegh Guldberg et al., 2018) arising from three main sources (Deser, Knutti, et al., 2012; Deser, Phillips, et al., 2012): (i) anthropogenic greenhouse gases emission forcing (scenario uncertainty from here on), which reflects the unknowns regarding the policy and technological developments in the future; (ii) numerical climate models (model uncertainty), which are the result of imperfect understanding of climate dynamics, that leads to assumptions, simplification and parameterizations in the physics built into climate models; and (iii) natural internal climate variability (stochastic uncertainty), which is a measure of the inherent randomness of climate occurrences and is intrinsic to climate processes (e.g., Deser, 2020). Unlike scenario and model uncertainty, stochastic uncertainty is considered irreducible (e.g., Fatichi et al., 2016), that is, it will persist despite advances in scientific knowledge and prediction tools. In the case of hydrological projections, there are additional sources of uncertainties beyond the influence of climate variables. These include, for example, the difference among hydrological models (e.g., Addor et al., 2014), their parameterization (e.g., Feng & Beighley, 2020), or the hydrological effects induced by changes to land use and landscape (e.g., Chawla & Mujumdar, 2018) and other anthropogenic interventions (e.g., Magilligan & Nislow, 2005).

The relative contribution of each factor depends on spatial and temporal scales, the time horizon of the analysis, and the examined variable. For example, at local scale while stochasticity dominates the uncertainty in precipitation, temperature uncertainty is mostly driven by climate model and scenario uncertainties (Fatichi et al., 2015, 2016). In general, stochastic uncertainty is relatively larger when looking at the near future (a few decades), thus suggesting a limited potential for uncertainty reduction for shorter lead times (Hawkins & Sutton, 2011). Whereas its contribution increases with finer temporal and spatial resolution (Addor et al., 2014; Fatichi et al., 2014, 2016; Hawkins & Sutton, 2011; Peleg et al., 2019). In contrast, scenario uncertainty plays a dominant role in the projection of temperature changes for long-term horizons because of the large influence of greenhouse gas emissions on global temperatures (Hoegh Guldberg et al., 2018).

These climate uncertainties propagate further down the model chain and affect response of catchments in future climate scenarios, as shown by numerous works that have studied the magnitude and partitioning of hydrological uncertainties, including the uncertainty introduced by the use of hydrological models (e.g., Chawla & Mujumdar, 2018; Chen et al., 2017; Clark et al., 2016; Feng & Beighley, 2020; Vetter et al., 2017). An important study of hydrological uncertainty estimation in mountain areas was presented by Addor et al. (2014), who used a simulation ensembles approach to quantify and partition uncertainties of annual streamflow in six alpine catchments while comparing the outputs of three different hydrological models. They show that, as seen in larger-scale studies, most of the uncertainty in future streamflow prediction arises from climate models

and natural climate variability, with only a small influence of scenario uncertainty or the choice of hydrological model for long-term horizons (end of the century).

Quantifying the contribution of each of these uncertainty sources, known as uncertainty partitioning, is therefore fundamental for understanding the potential for making more accurate hydrological projections. A major challenge, however, is that large ensembles of simulations are required to explore the range of natural climate variability. Climatic modelling is based on General Circulation Models (GCMs), or Regional Climate Models (RCM), which solve physically-based equations to simulate the climate of the past and future. An important limitation is that, due to their large computational requirements, the product of GCMs or RCMs usually consists of a single or at most few realizations of future climate variables, which means that an assessment of natural (stochastic) climate variability is generally not straightforward (Hawkins & Sutton, 2009, 2011). The few existing exceptions (e.g., Deser, 2020; Deser, Knutti, et al., 2012; Lehner et al., 2020; Thompson et al., 2015) have produced results of coarse resolution, which are not suitable for hydrological modelling at a broad range of catchment scales (Fatichi et al., 2015).

This deficiency can be overcome by simulating many possible realizations of a future climate at the right scale for hydrological modelling with stochastic weather generators (WG). By forcing a WG to follow the climate conditions estimated by GCMs or RCMs, it is possible not only to reproduce small-scale future climate variables but also to obtain an ensemble of simulations for uncertainty quantification. Using deterministic hydrological models forced by WG simulations allows to estimate future hydrological statistics, assess their variability, partition the different sources of uncertainties, and quantify the potential for narrowing the uncertainty down. Some examples in using WGs to quantify sources of uncertainty include, among others, Minville et al. (2008), who combined a WG with a hydrological model to partition the uncertainty of climate change impacts on a catchment in northern Canada and found that the choice of climate models has a larger effect on the assessed impacts than the selected emission scenario. Fatichi et al. (2015) used multisite rainfall and temperature generators to study the hydrological response of the Upper Rhone basin, showing how the impact of uncertainty is reduced for heavily regulated catchments and is highest for catchments fed predominantly by liquid precipitation. Likewise, Camici et al. (2017) used a rainfall generator and hydrological model chain to examine hourly discharge extremes in the upper Tiber basin, in Italy, and highlighted the influence of catchment permeability on the response to climate change; also showing that natural variability is a much larger driver of uncertainty than climate models. In general, these and other studies agree that stochastic and climate model uncertainties are the two most relevant uncertainty sources for streamflow projections (see also Chawla & Mujumdar, 2018; Gao & Booij, 2020; Giuntoli et al., 2018; Shen et al., 2018). Accordingly, this work focuses on analysing those two uncertainty sources, omitting the effects of emission scenario and hydrological-model uncertainties.

While the scale dependency and spatial and elevation variability of climate change impacts on hydrology have been previously studied,

the uncertainty of those projections has not received the same level of attention. This study aims to address this knowledge gap and to do so at the seldom explored sub-catchment and hourly scales. Consequently, we address here three specific research goals: (i) to quantify the uncertainty of changes on distributed climatic and hydrological variables at sub-catchment scales, and determine their relation with elevation; (ii) to estimate the fraction of stochastic and climate model uncertainty in the future projections, and thus show the importance of natural variability when assessing climate impacts; and (iii) to assess the potential for narrowing down the uncertainty of streamflow extremes projections by estimating their signal-to-noise ratio and quantifying the magnitude of the irreducible stochastic uncertainty.

To this effect, we present in the following sections an experimental framework based on the work presented in Moraga et al. (2021), which consists of combining the use of a two-dimensional stochastic weather generator, AWE-GEN-2d (Peleg et al., 2017, 2019), with a distributed hydrological model, TOPKAPI-ETH (Fatichi et al., 2015) to generate ensembles of climate and hydrological variables characterizing the present climate and, based on the outputs of nine GCM-RCM modelling chains, their response to climate change throughout the 21st century. This framework allows us to go beyond previous studies as we quantify the contribution of stochastic uncertainty on an array of climate and hydrological variables—including extreme events—at considerably high resolution in space. Thus, we provide a reference for quantifying and partitioning uncertainty related to the effects of climate change on catchment hydrology.

2 | METHODS AND DATA

2.1 | Study area

The numerical experiments are based on data from two Swiss mountainous catchments: Kleine Emme and Thur. The Kleine Emme is located in the northern Alpine region in central Switzerland and extends over an area of 478 km². Its mean elevation is 1047 m, and highest elevation is 2330 m, and its outlet is at 438 m near the city of Lucerne. It receives mean annual precipitation of 1650 mm year⁻¹, has an average temperature of 7°C and its outlet discharges on average 12.6 m³ s⁻¹ (833 mm year⁻¹). The Thur river catchment, while part of the greater Alpine area, is mostly located in the Swiss plateau physiographic division in northeast Switzerland. It has an area of 1730 km², a highest point of 2434 m, a mean elevation of 773 m, and a lowest point at 361 m in the town of Andelfingen. The mean annual precipitation over the Thur catchment is 1350 mm year⁻¹, an average temperature of 8.4°C and the average streamflow at the outlet is 46.7 m³ s⁻¹ (851 mm year⁻¹). A particular feature of these catchments is that they do not have major stream regulations, water extractions, or large urbanized surfaces, and the prevalent land cover is cropland and natural pasture. A summary of their location, elevation map, and elevation distribution is presented in Figure S1.

The topography of the catchments was characterized using a regular grid with a cell size of 100 m × 100 m, based on topographic information obtained from a digital elevation model (SwissTopo, 2002). Soil

properties, used to assign hydraulic soil parameters as well as soil depth, were determined from the soil map of Switzerland (Bodeneignungskarte, 2012). Likewise, the Corine dataset (CLC, 2012) was used to derive land cover classifications to determine surface roughness and evapotranspiration parameters.

2.2 | Models and data

The two-dimensional weather generator AWE-GEN-2d (Peleg et al., 2017, 2019) was used to simulate gridded climate variable time series at a high spatial (2 km for precipitation, 100 m for the other variables) and temporal (5 min for precipitation, hourly for the other variables) resolutions. Among its features, AWE-GEN-2d is capable of realistically modelling the arrival process of storms as well as their spatiotemporal evolution based on ground stations and weather radar observations. Satellite images are used to calibrate the cloud cover module (cross-correlated with the precipitation fields), which in turn controls the distributed incoming shortwave radiation. Furthermore, the advection of cloud and precipitation fields was estimated based on statistics of geostrophic wind velocities obtained from reanalysis data, with the Cartesian components of convection modelled as a bivariate autoregressive process at a 5 min resolution. Near-surface air temperature is characterized as a stochastic process using modelled incoming long-wave radiation and the previous hour air temperature as inputs, and is distributed in space via a stochastic lapse rate, with the capability to reproduce thermal inversion events. AWE-GEN-2d was calibrated using a large dataset of climate observations and validated by analysing statistics not used in the calibration process, as described in Peleg et al. (2017a), where a comprehensive description of the model structure is provided.

The hydrological simulations were performed using TOPKAPI-ETH (Fatichi et al., 2015), a distributed hydrological model, suitable for characterizing surface and sub-surface processes at high resolutions (sub-kilometre grids) and efficient enough to use for long simulations in relatively large domains. As such, it has been employed successfully to model the hydrological response of a number of mountainous catchments (e.g., Battista, Molnar, & Burlando, 2020; Battista, Schlunegger, et al., 2020; Fatichi et al., 2014; Moraga et al., 2021; Pappas et al., 2015; Paschalis et al., 2014). With precipitation, temperature and cloud transmissivity as input, the model simulates a broad range of hydrological variables including streamflow, snowmelt, soil moisture, groundwater flows, and evapotranspiration. It models surface and sub-surface flows through two soil layers plus a groundwater compartment by approximating lateral water transfer with the kinematic-wave equation following topographic gradients (Liu & Todini, 2005). Infiltration capacity is explicitly computed at each grid cell and surface runoff may occur due to either infiltration excess or saturation of the upper soil layer. Additionally, potential evapotranspiration is calculated with the Priestley–Taylor equation (Priestley & Taylor, 1972) as a function of incoming shortwave radiation, albedo, and temperature.

Climate observations from an array of sources were used as a model forcing and for calibration. As required by AWE-GEN-2d, point temperature, precipitation and radiation observations at hourly

resolution were obtained from ground stations operated by MeteoSwiss, who also provided the gridded daily datasets for temperature and precipitation at 2-km resolution, (MeteoSwiss, 2016; Wüest et al., 2009), as well as C-band weather radar information used to characterize the spatial structure of rainfall (Germann et al., 2006). Geostrophic wind velocity, used to model the advection of storm cells, as well as cloud cover, were extracted from the MERRA-2 reanalysis dataset (Rienecker et al., 2011). The temperature and precipitation statistics from nine different GCM-RCM model chains, developed in the context of the EURO-CORDEX initiative (Jacob et al., 2014; Kotlarski et al., 2014), and later post-processed by MeteoSwiss (CH2018, 2018), were used to re-calibrate AWE-GEN-2d parameters for future climate following the procedure described in Peleg et al. (2019).

The calibration of TOPKAPI-ETH was based on hourly observations of streamflow at the outlet of the catchments, which were provided by the Swiss Federal Office for the Environment (FOEN). The model was manually calibrated by optimizing the Nash-Sutcliffe Efficiency statistic (NSE) at the catchments' outlet at the hourly (NSE of 0.64 at the Kleine Emme and 0.60 at the Thur) and monthly (0.76 and 0.78) scales for the 2000–2009 period, as detailed in Moraga et al. (2021).

2.3 | Design of the experiment

The experiment aimed to generate a large enough dataset of simulated variables, representing different climate trajectories, to allow for

the quantification of uncertainty in the resulting climate and hydrological variables. The numerical experiment consisted of three parts, schematized in Figure 1 and detailed in the following sections: the generation of present and future climate ensembles following multiple climate trajectories, the simulation of high-resolution hydrological variables, and the quantification of changes and associated uncertainties. The procedure to obtain the statistics for extreme events is also explained in Section 2.3.4.

2.3.1 | Ensembles of climate variables

AWE-GEN-2d was first used to simulate 15 realizations of 30-year-long time series (equivalent to 450 years) of variables that characterize the period 1976–2005 (present climate). To simulate the future climate variables, the climate change signals were obtained from the results of RCM transient simulations: nine different climate trajectories (Model chains) were used (Table S1), all of which follow the RCP 8.5 emission scenario.

The Factors of Change approach (FC, e.g., Fatichi et al., 2011) was used to re-parameterize the temperature and precipitation parameters until the end of the 21st century. Unlike direct forcing methods, the factors of change (also called delta-change) approach does not deal with the issue of biases in the RCM outputs, as it implicitly assumes that any bias affects similarly both the control and future scenarios (Anandhi et al., 2011; Lenderink et al., 2007; Rasmussen et al., 2012; Teutschbein & Seibert, 2012; van Roosmalen et al., 2011). The procedure consists, in the case of temperature, in

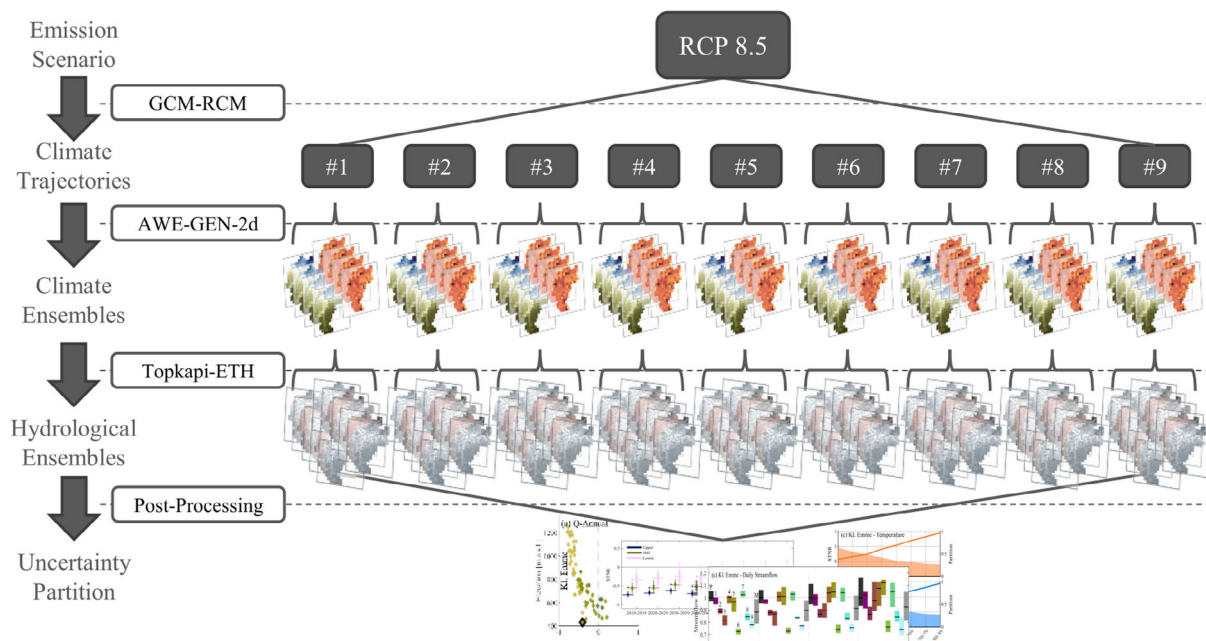


FIGURE 1 Schematic representation of the numerical experiment used to quantify and partition uncertainty. Nine climate model outputs, which follow an RCP 8.5 emission scenario, are stochastically downscaled to produce ensembles of climate variables, which in turn feed a deterministic hydrological model. The large array of climate and hydrological results are post-processed to quantify the uncertainty in the climate and hydrological projections and to compute the uncertainty partition

obtaining the difference in monthly means between the control period and future climate RCM outputs and subsequently applying the additive factor to the temperature simulated by the WG. In the case of precipitation, the objective is to obtain the ratio between future and present daily precipitation mean and other statistics, so as to follow not only the change in average precipitation, but also in higher order statistics (as in Fatichi et al., 2016; Peleg et al., 2019). To do this, the control and future RCM outputs are compared at the monthly level to extract the changes in mean, standard deviation, and kurtosis of daily precipitation using a moving average with a 30-year window and a 10-year shift. These changes are then forced onto the present-climate statistics so as to ensure that they are reflected in the estimation of the new WG parameters and consequently on the future climate simulations. In total, ensembles consisting of ten realizations of 80 years (2010–2089) for each of the nine climate trajectories were simulated, for a total of 7200 years of time series representing the future.

2.3.2 | Hydrological simulations

The hydrological processes in the present and future for the Thur and Kleine Emme catchments were modelled using TOPKAPI-ETH. The climate inputs for the simulations were obtained from the previously described outputs of the weather generator. Specifically, ensembles of gridded time series of 2 km and hourly resolutions for precipitation, air temperature, and cloud transmissivity were fed to the model to perform multiple realizations of continuous hydrological simulations for the present and future climates.

The hydrological outputs consisted of gridded datasets at 100 m and hourly resolutions for variables that represent the main components of the hydrological budget: streamflow, rainfall, snowmelt, evapotranspiration, and change in soil water storage. Outputs were stored not only for the catchment scale at the outlet of the river, but also at the scale of small sub-catchments along the river networks: 97 virtual stations were selected in the Kleine Emme and 112 in the Thur catchments for this purpose. The selected variables, the number of sub-catchments, and the size of the simulation ensembles represent a compromise between obtaining large and comprehensive enough datasets for the proposed uncertainty partition analysis and manageable size of data storage.

2.3.3 | Quantifying uncertainty

The third part of the experiment refers to the processing of simulation results to quantify the uncertainty source in the simulated variables. Based on the concept of signal-to-noise ratio (STNR; Fatichi et al., 2014; Hawkins & Sutton, 2009, 2011), we summarize the magnitude of the uncertainty by means of a proposed STNR statistic, which we define as the ratio between the change in the median values of a given statistic for a given variable q (e.g., extreme streamflow, mean rainfall) between future and present climate (the signal) and the spread measured by the average interquartile range IQR (the noise)

around the median of the future and present simulation ensembles, computed considering only the stochastic variability, that is:

$$\text{STNR} = \frac{\text{Signal}}{\text{Noise}} = \frac{2 \times (q_{50}^{\text{fut}} - q_{50}^{\text{pres}})}{\text{IQR}_{\text{fut}} + \text{IQR}_{\text{pres}}} \quad (1)$$

Absolute values of STNR larger than 1 indicate that the magnitude of the signal lies outside of the average natural variability of 50% of the sample (IQR is computed between the 25th and 75th percentiles) and is assumed to represent a robust change in that statistic. Conversely, absolute STNR values smaller than 1 imply that the change is comparable or smaller than the natural variability represented by 50% of the sample. The sign of STNR is given by the direction of the signal, thus positive values indicate an increase of the analysed variable in the future.

The resulting variable uncertainty can be partitioned into two contributing factors (Hawkins & Sutton, 2011) namely, the internal climate variability and the climate model uncertainty. Internal climate variability represents stochastic uncertainty and is calculated as the mean of the interquartile ranges (IQR) from all climate trajectories (models) in the ensemble:

$$U_{\text{ICV}} = \frac{\sum_1^N \text{IQR}_n}{N} = \frac{\sum_1^N (q_{75n} - q_{25n})}{N} \quad (2)$$

where N is the total number of climate trajectories (equal to the number of climate model chains) in the ensemble. The climate model uncertainty was computed as the interquartile range of the means obtained for each climate trajectory, averaging the stochastic replicates:

$$U_{\text{CM}} = \text{IQR}(\{\mu_1, \mu_2, \dots, \mu_n, \dots, \mu_N\}) \quad (3)$$

where μ_n is the mean of the selected variable for trajectory n . As such, the relative importance P of uncertainty attributed to each contributing factor is obtained as:

$$P_{\text{ICV}} = U_{\text{ICV}} / (U_{\text{CM}} + U_{\text{ICV}}); P_{\text{CM}} = U_{\text{CM}} / (U_{\text{CM}} + U_{\text{ICV}}) \quad (4)$$

2.3.4 | Estimation of hydrological extremes

The analysis of extreme event statistics presented in Section 3.3 was performed by selecting the annual maximum streamflow (hourly or daily) for each of the 30 years of continuous simulations representing the present (1976–2005) and end-of-the-century (2060–2089) climate, and then fitting the annual maxima with a Generalized Extreme Value distribution (GEV, Jenkinson, 1955).

Return periods ranging from 2 to 25 years were computed for each of the 15 realizations simulated for the present climate and the 10 realizations simulated for each of the 9 future trajectories (see Section 2.3.1). These 15 and 9×10 estimated return periods

compose the data sample from which the STNR and uncertainty partition were quantified as described in Section 2.3.3.

3 | RESULTS

The proposed framework allows for the quantification of uncertainty and its partition not only for several variables of interest in hydrological practice, but also across spatial and temporal scales. First, the STNR and partition of stochastic and climate model uncertainties for distributed climate variables are presented in Section 3.1. Then, Section 3.2 is dedicated to the hydrological variables, including streamflow and the main components of the hydrological budget in the various sub-catchments. Finally, Section 3.3 shows the computed STNR and fraction of stochastic uncertainty for the changes in extreme high flows.

3.1 | Uncertainty in climate projections

For both catchments, the expected values for each grid cell (ordered by elevation) in total precipitation (including liquid and solid phases) and near-surface air temperature are shown in Figure 2. Annual precipitation shows a non-trivial change pattern, as the higher parts of the catchments are expected to experience a decrease in precipitation in the Kleine Emme (Thur) of up to 11% (9%) whereas the drier, lower parts of the catchments will see an increase in projected precipitation by 10% (17%), for an overall change of -3.2% ($+1.4\%$). Conversely, the projected changes in temperature are more homogeneous, with

progressive catchment-average increases that reach 4.2°C at the Kleine Emme and 4.0°C at the Thur catchments by the end of the century.

In turn, the STNR and uncertainty partition of precipitation and temperature, computed using the end-of-century decade (2080–2089) and present climate simulations (1976–2005), show that, for both the Kleine Emme (Figure 3a) and Thur (Figure 3e), the signal of change in precipitation is weaker than the noise, as shown by the magnitude of STNR values with ranges between -0.56 and 0.57 in Kleine Emme, and between -0.51 and 0.89 in Thur. It is possible to observe clear spatial patterns that follow those of the overall change in precipitation predicted by the climate models (see Moraga et al., 2021), with negative values of STNR at higher elevations, in the southern part of the catchments, and positive values at lower elevations. Most of the uncertainty is explained by the stochastic uncertainty, with its share of the total uncertainty ranging between 53% and 79% for Kleine Emme (Figure 3b) and between 57% and 91% for Thur (Figure 3f). Moreover, there is a strong negative correlation between elevation and the share of uncertainty associated with stochastic variability in precipitation in the Kleine Emme (linear regression with $R^2 = 0.65$), but not in the Thur catchment ($R^2 = 0.02$).

The large increase in average temperatures is reflected in the STNR, with values ranging between 3.98 and 4.85 in the Kleine Emme (Figure 3c) and between 2.81 and 6.05 in the Thur (Figure 3g), which confirm a robust change signal. Unlike for precipitation, the uncertainty is spatially uniform, with ranges narrower than 1% for both catchments, and is mostly explained by climate model uncertainty: 73% of the total in the Kleine Emme (Figure 3d) and 65% in the Thur (Figure 3h). This becomes clearer in Figure S2, as the stochastic

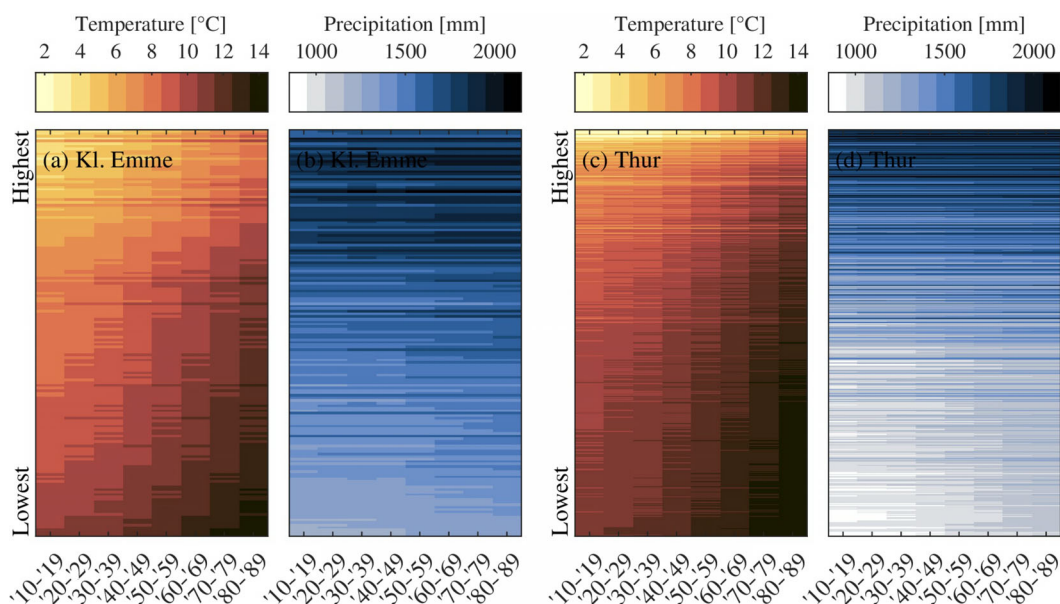


FIGURE 2 Temperature and precipitation values throughout the future climate simulations for each of the 160 grid cells in the Kleine Emme (a, b) and 497 in the Thur (c, d) river catchments. Each row represents a grid cell ordered from highest to the lowest elevation and the colours represent the decadal means

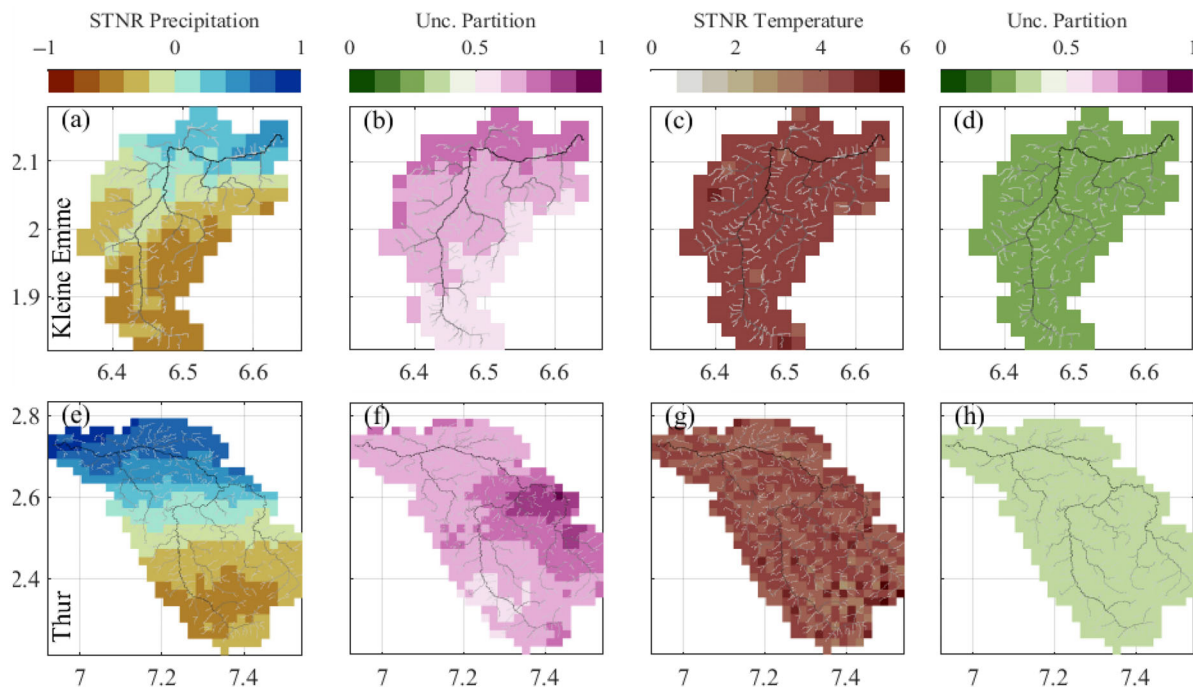


FIGURE 3 Signal-to-noise ratio (STNR) and uncertainty partition (share of stochastic uncertainty) of precipitation and temperature by the end of the century (2080–2089) in the Kleine Emme (a–d) and Thur (e–h) catchments. The coordinates in UTM 32 N and 10^6 meters, and the river network are superposed over the rasters

uncertainty for each future climate trajectory is indeed very narrow, and the overall uncertainty observed in the multi-model mean is small compared to the expected temperature change in the order of 4°C .

3.2 | Uncertainty in hydrological projections

The total uncertainty attributed to natural climate variability (stochasticity) and climate models was computed for the hydrological components at the seasonal scale, following the procedure detailed in Section 2.3.3. Most of the uncertainty in streamflow projections (Figure 4a,c) is explained by stochastic uncertainty, although it can vary considerably across seasons from 58% to 83% in the Kleine Emme and from 68% to 74% in the Thur, with the largest difference between the two catchments being spring flows, as 81% of the uncertainty is explained by stochasticity in the Thur and only 64% in the Kleine Emme. At the annual scale (not shown), stochasticity explains 56% of future streamflow uncertainty in Kleine Emme and 73% in Thur, mostly due to the high uncertainty in liquid precipitation.

The uncertainty partition of specific components of the hydrological cycle are shown in Figure 4b,d. Spring snowmelt, which is a process largely driven by temperature, is the most sensitive component to climate model uncertainty, which accounts for 50% of uncertainty in the Kleine Emme and 40% in the Thur. However, its contribution to the hydrological response is expected to decrease drastically by the end of the century, to the point that its uncertainty range becomes too small to influence streamflow considerably (on average, spring snowmelt will represent only 15% and 22% of total spring streamflow,

respectively). In contrast, evapotranspiration plays an important role in the hydrological response, especially during summer (JJA) at the Thur catchment, with trimestral contributions of around 250 mm, but its uncertainty range is relatively narrow compared to that of liquid rainfall. Furthermore, its uncertainty partition indicates that it is also mostly driven by stochasticity, which suggests a large influence of summer precipitation rather than temperature on the total evapotranspiration fluxes.

The evolution of the STNR and the fraction of stochastic uncertainty throughout the 21st century are shown in Figure 5. While the absolute values in the STNR of streamflow for both catchments remains relatively constant and low, the partition of the uncertainty shows different progressions. In the Kleine Emme, the fraction assigned to internal climate variability decreases from around 90% in the early 21st century to under 60% by the end of it, whereas in the Thur it remains constant at around 75%. The combination of low STNR values for the end-of-century streamflow projections, combined with a high contribution of stochastic uncertainty, clearly suggest that high uncertainties in streamflow projections will persist even if perfect climate models were available.

The driving climate variables, temperature and precipitation, show similar behaviours in both catchments, with a clear decrease in the uncertainty related to internal climate variability, which shows the increasing importance of climate models with longer simulation times.

The distributed hydrological simulations allow extending the uncertainty analysis to the sub-catchment scale by computing the STNR at multiple points throughout the catchments for key hydrological variables. Figure 6 shows the relation between sub-catchment

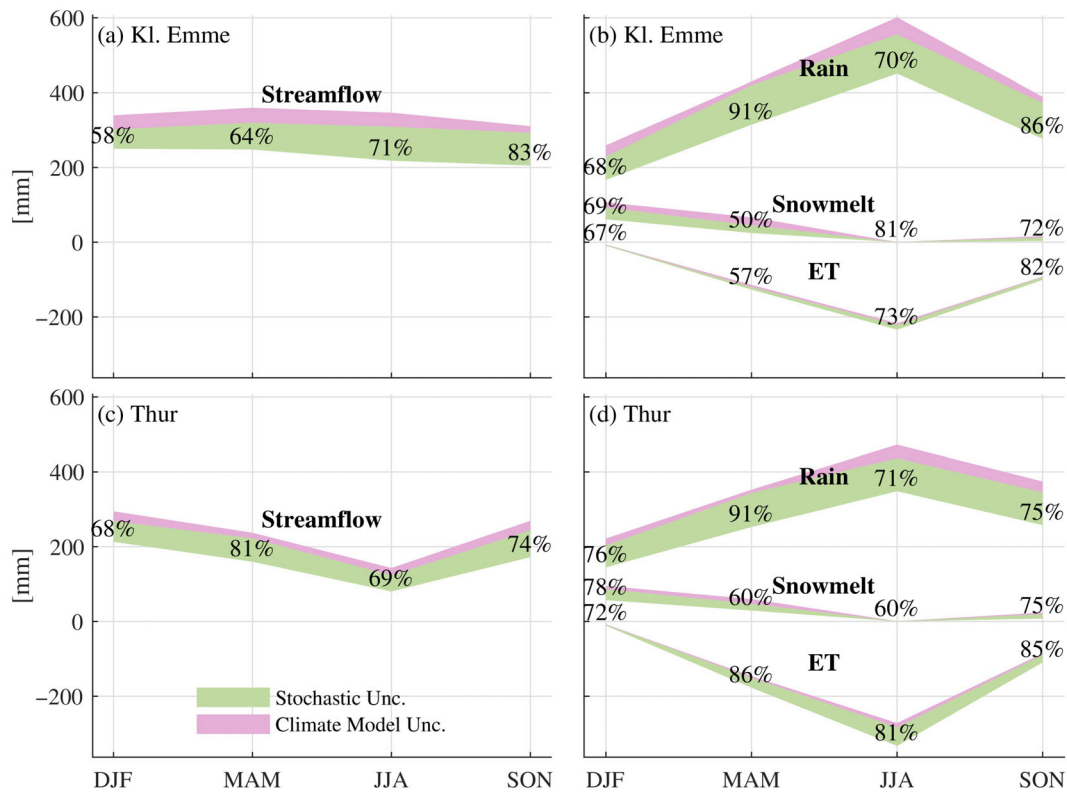


FIGURE 4 Future stochastic and climate model uncertainty for streamflow (a, c) and the main hydrological components (b, d): Evapotranspiration (ET, presented as a negative value), rainfall, and snowmelt at the seasonal scales in the Kleine Emme (a, b) and Thur (c, d) river catchments. The vertical axis represents the amount of water in mm over the season attributed to each hydrological component with corresponding uncertainty source, and the percentages indicate the fraction of uncertainty attributed to internal climate variability (stochastic uncertainty)

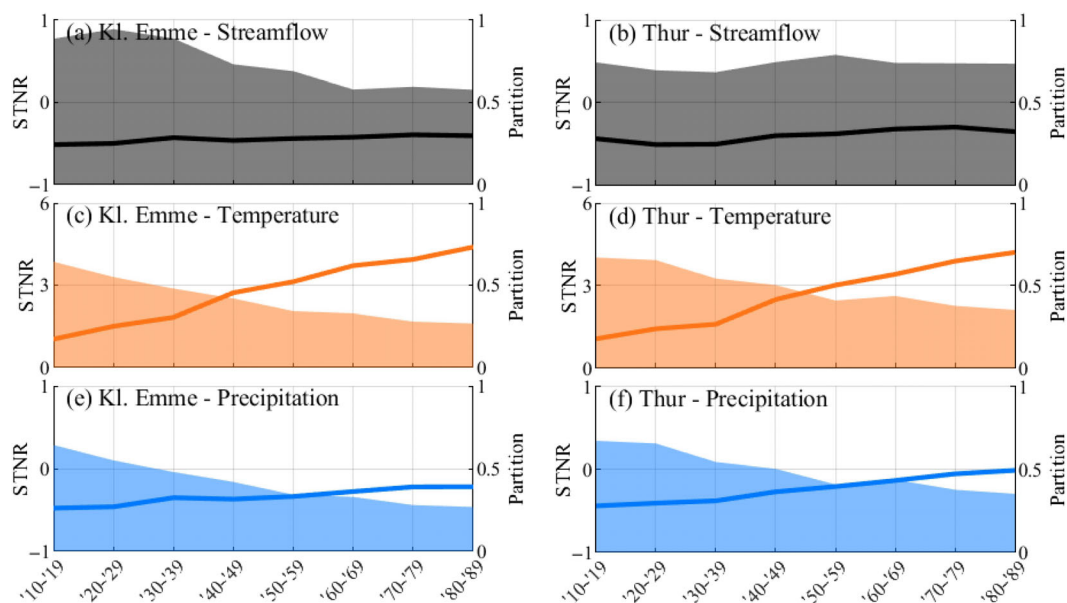


FIGURE 5 Temporal evolution of the signal-to-noise ratio (solid lines) and partition of uncertainty attributed to stochasticity (shaded areas) for streamflow at the outlet of the catchments (a, b), mean temperature (c, d), and mean precipitation (e, f) throughout the simulation period for the Kleine Emme and the Thur river catchments

elevation, the STNR of seasonal and annual hydrological statistics at the end-of-the-century, as well as the uncertainty partition. As reported by Moraga et al. (2021), the change in mean annual

streamflow in a future climate exhibits an inverse correlation with elevation. However, the results here show that this change is not statistically strong, as the STNR is lower than one for virtually all sub-

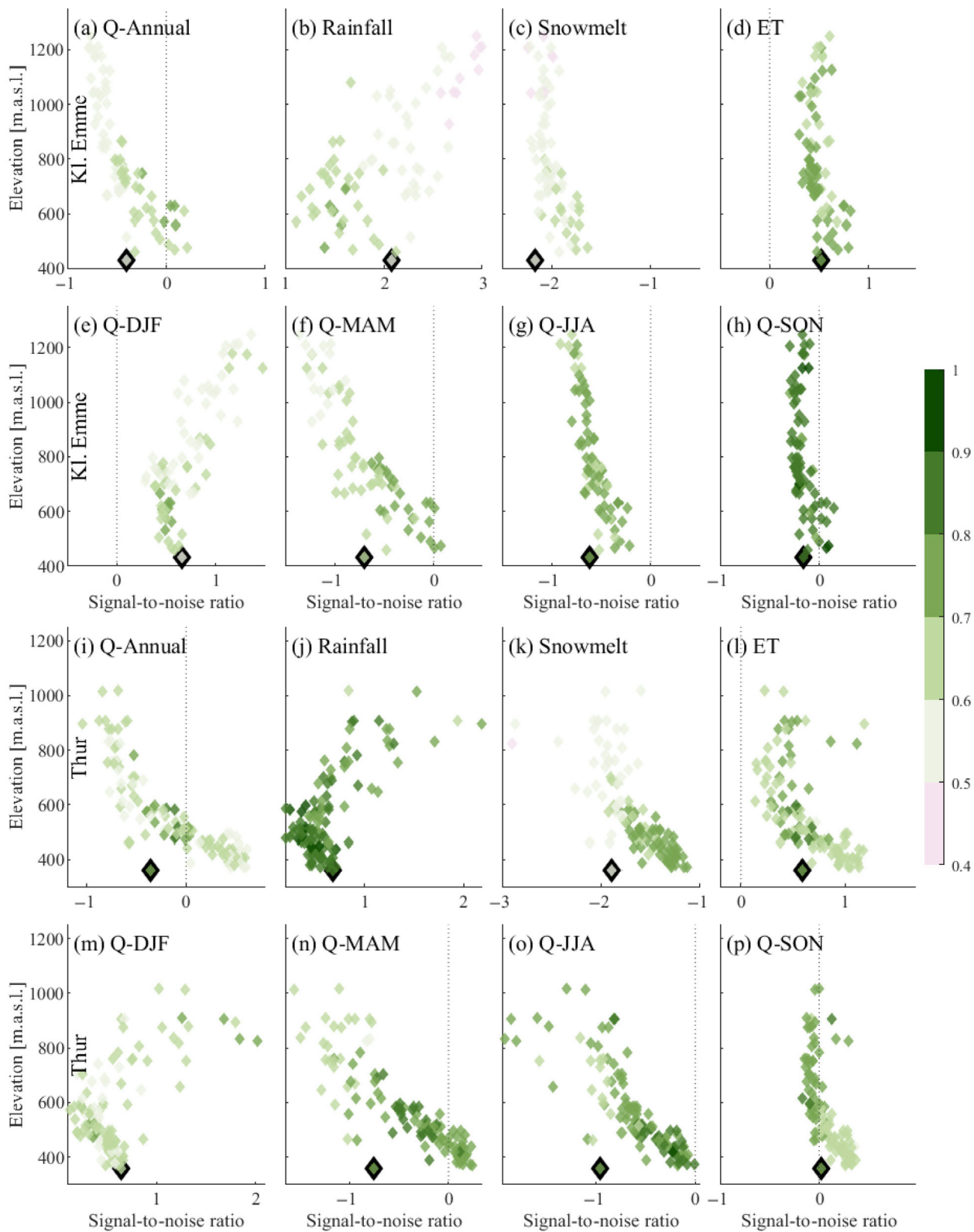


FIGURE 6 Signal-to-noise ratio (STNR) of key hydrological variables in the Kleine Emme (a–h) and Thur (i–p) catchment. The subplots show the scatter plot between STNR (comparing end-of-the-century multi-model mean and present climate simulations) of the mean three-month season flows and the elevation of the sub-catchment's outlet. The outlined symbol is the outlet of the entire catchment. The colours in the markers show the fraction of uncertainty attributed to the natural climate variability

catchments, indicating a signal of change smaller than the noise (Figure 6a,i), mostly due to stochastic uncertainty. Furthermore, both study sites exhibit a clear and similar negative correlation between sub-catchment elevation and the STNR value.

The change signals for individual hydrological components are clearer than for the overall streamflow. The signal of rainfall, for example, is larger than the noise (and positive in sign) for all the sub-catchments in the Kleine Emme and for the highest ones in the Thur (Figure 6b,j, respectively), also showing a clear positive correlation with elevation. The partition of stochastic uncertainty for rainfall is higher at the Thur (between 67% and 95%) than at the Kleine Emme (45%–79%), and the model uncertainty becomes more relevant at higher elevations. Likewise, the STNR for snowmelt reduction shows high absolute values (Figure 6c,k). In Kleine Emme, values range between -2.2 and -1.6 , and the fraction of stochastic uncertainty goes from 48% to 64%. In the Thur, STNR is negatively correlated with elevation and ranges between -2.9 and -1.1 , and the stochastic uncertainty is between 49% to 80%, with the lowest values corresponding to the highest sub-catchments. For evapotranspiration, the partition of stochastic uncertainty fluctuates around 70% for all elevations (between 63% and 78% in Kleine Emme, and between 60% and 87% in Thur) with an overall weak positive STNR (<1) for all the sub-catchments in Kleine Emme and for 85% of sub-catchments in Thur.

Because of their different importance in the total response, the influence of these hydrological components on the overall uncertainty of streamflow needs to be weighted by their respective contribution to the hydrological budget. As seen in Figure 4, rainfall plays the largest role in the hydrological budget, thus suggesting that its large stochastic uncertainty is responsible for most of the uncertainty in streamflow, which explains the predominance of stochastic uncertainty over climate model uncertainty for streamflow projections. Snowmelt is, conversely, the hydrological component that is most sensitive to temperature and, therefore, to climate model uncertainty. Nonetheless, internal climate variability takes an equal or slightly larger share of its uncertainty partition (Figure 4i,j). This means that the amount of precipitation, driven mostly by stochastic uncertainty, is as relevant to the uncertainty of snowmelt as temperature, which is driven mostly by climate model uncertainty, likely due to the role played by precipitation on snow accumulation.

In contrast with the weak STNR magnitudes of annual streamflow, the projections of seasonal flows show stronger signals, particularly in the highest sub-catchments. Winter flows (Figure 6e,m) show a positive STNR, which is positively correlated with elevation, as winter rainfall will increase at higher altitudes. Spring (MAM) and Summer (JJA) flows, which are influenced by snowmelt, show the opposite behaviour, with negative STNR values which are negatively correlated with elevation. The highest partition for stochastic uncertainty is found in the lower reaches of the river networks.

3.3 | Uncertainty in future hydrological extremes

The large simulation ensembles allow investigating changes in the frequency of occurrence of extreme hydrological events and analysing

the relative importance of climate model and stochastic uncertainties. Figure 7 shows the uncertainty of the annual maximum discharge for return periods between 2 and 25 years and for both hourly and daily resolutions. From the plots, dissimilar trends for both catchments can be observed at different return periods and resolutions. In general, the magnitude of uncertainty is high, especially for hourly extreme streamflow, and as expected, it increases with higher return periods: for the hourly extremes, the uncertainty range changes from -16% to -6% for the 2-year return period to -13% to 4% for the 25-year return period in the Kleine Emme and from -8% to $+4\%$ for $T = 2$ years to -14% to $+19\%$ for $T = 25$ years in the Thur. Although it is apparent that climate model uncertainty is relevant, as evident from the difference among the medians of the different climate trajectories (shown with grey bars), most of the uncertainty is again explained by the stochastic uncertainty. According to the multi-model mean, both hourly and daily streamflow maxima in the Kleine Emme will become slightly smaller, even though with a large uncertainty range. The results for the Thur show, conversely, no clear change signal for hourly extremes, and a small decrease in daily extremes.

Extreme streamflow statistics were also computed for every sub-catchments of both river basins. Figure 8 shows that the STNR for maximum hourly and daily flows has absolute values well below one for all sub-catchments, thus highlighting the large uncertainty in the projection of hydrological extremes into the future with a slight decrease of daily extreme streamflow at high elevations. As before, stochasticity is the dominant source of uncertainty, with average values in the Kleine Emme of 76% (81% in the Thur) for hourly maximum, and 72% (76% in the Thur) for daily maximum. The large relative importance of stochasticity, combined with weak change signals, points to a very limited potential for providing more accurate projections of hydrological extremes.

4 | DISCUSSION

We have presented a framework that, by combining the use of a weather generator and a distributed hydrological model, allowed us to project future climate and hydrological variables at high resolution, estimate their STNR and the contribution of two major uncertainty sources: stochastic (internal climate variability) and climate model uncertainty. While we explored those two uncertainty sources due to their higher relevance to hydrological projections, this framework can easily be extended to quantify the partition of uncertainty due to emission scenarios—to which the temperature-driven processes are very sensitive—or to other uncertainty sources, such as hydrological model uncertainty, which does not appear to contribute considerably to the total uncertainty in the Alpine region (Addor et al., 2014), but can be a major factor in other climate re (e.g., Giuntoli et al., 2018).

The projections for mean streamflow are characterized by low STNR values and a large contribution of stochastic uncertainty (Figures 4–6). This contrasts with studies on larger domains (as well as regional scales), that conclude that GCMs have a larger influence on future uncertainty than internal climate variability (e.g., Chawla and Mujumdar, 2018.; Gao & Booij, 2020; Giuntoli et al., 2018), but is

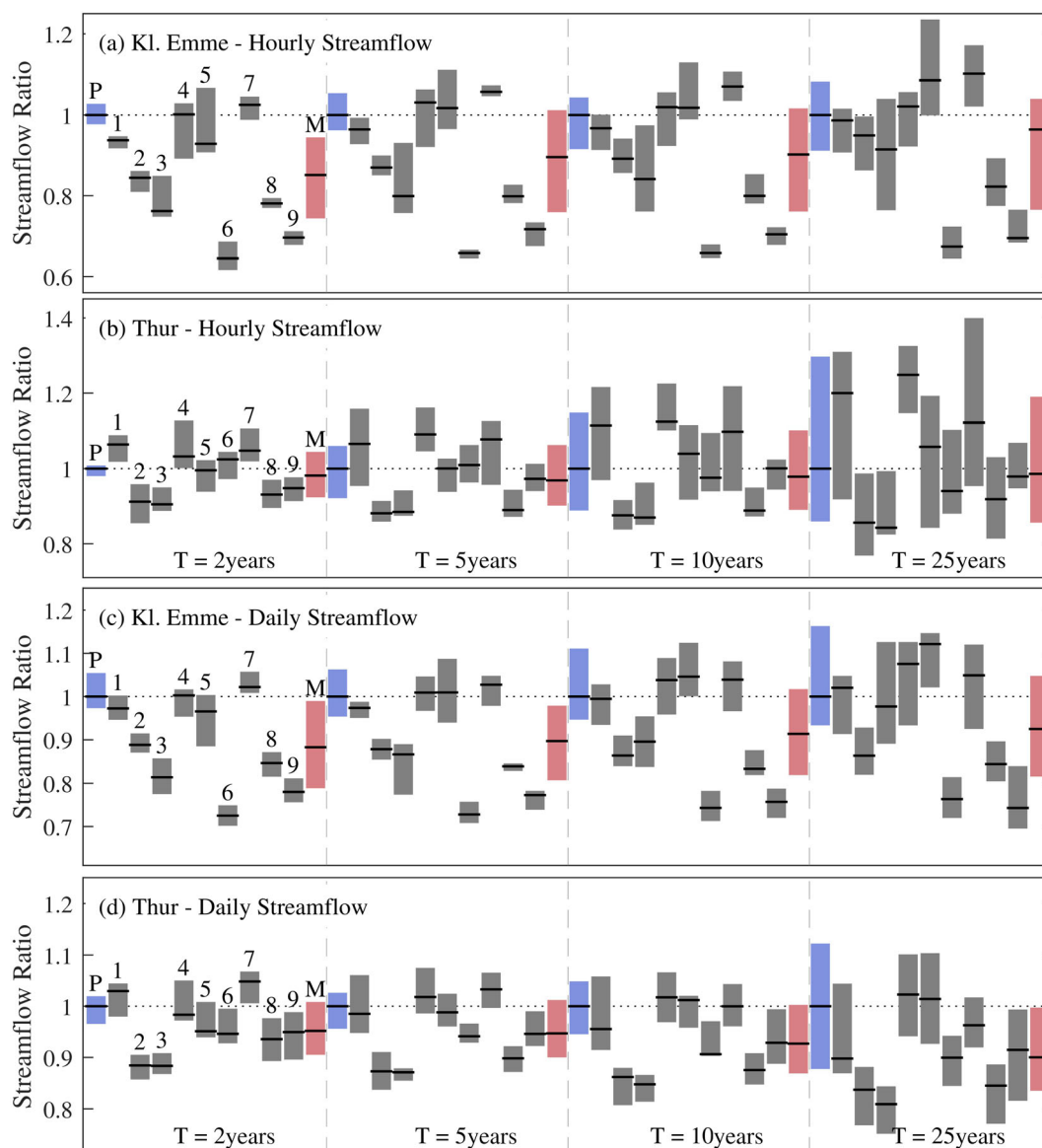


FIGURE 7 Annual maximum streamflow for a given return period for present and future climate (2060–2089) at the hourly (a, b) and daily (c, d) scales at the Kleine Emme (a, c) and Thur (b, d) catchment outlets. The values are normalized by the median of the present climate. P refers to the present climate, numbers 1 to 9 refer to the nine different climate models, and M refers to the multi-model mean. Central lines in the box plots represent the median of the values obtained from fitting the simulated ensembles of annual maxima to a GEV distribution, while the boxes represent the interquartile range

consistent with the expectation of an increment of the importance of stochasticity for smaller spatial scales (Addor et al., 2014; Fatichi et al., 2014, 2016; Hawkins & Sutton, 2011; Peleg et al., 2019). Furthermore, the large magnitude of stochastic uncertainty suggests that high uncertainties in streamflow projections at our study sites will persist even if perfect climate models were available.

In contrast, the analysis at the level of hydrological components reveals high absolute values of STNR for liquid precipitation (rainfall), particularly in the Kleine Emme, as well as for snowmelt, indicating robust change signals in the projections because of the influence of rising temperature on precipitation form and on snowmelt. The signals for a positive change in ET are also generally weaker than the noise,

although at low elevations in the Thur catchment the temperature rise will drive a significant ET increase. Just as the relative contribution of specific hydrological components can be large at the seasonal scale, so is their influence on the magnitude and partition of uncertainty in the resulting streamflow. For example, due to the high influence of (temperature-dominated) snowmelt, summer and spring flows (Figure 6) present a larger share of climate model uncertainties than the annual average flow, especially for sub-catchments at high elevations, where the share of climate model uncertainty approaches 60%. Consequently, an improvement in climate model predictions with reduced spread among models implies a potential for narrowing the uncertainty of snowmelt predictions and, thus, of total streamflow

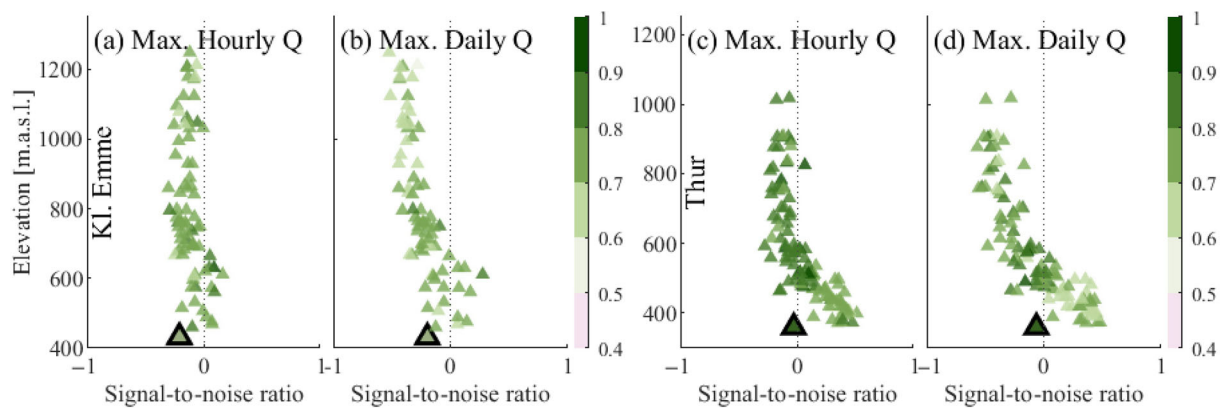


FIGURE 8 Signal-to-noise ratio (STNR) in the Kleine Emme (a–b) and Thur (c–d) catchment. The plots show the STNR (comparing end-of-the-century multi-model mean and present climate simulations) of hourly (a, c) and daily (b, d) maximum flows compared to the elevation of the sub-catchment's outlet. The outlined symbol is the outlet of the entire catchment. The colours in the markers show the fraction of uncertainty attributed to the internal climate variability

during warm seasons and at high elevations. Furthermore, this is a clear indication that other catchments in the alpine region should present a similar behaviour, i.e. that the climate model uncertainty is more important where the influence of snowmelt in the total hydrological budget is significant.

The projections for extreme high flows, summarized in Figures 7 and 8, reveal an uncertainty magnitude much larger than median climate change signal projected towards the end of the century. The vast majority of this uncertainty is again attributed to stochasticity rather than to climate model signals, in line with the findings of previous studies at different locations (Fatichi et al., 2014, 2016; Gao & Booi, 2020), thus suggesting that the improvement of climate models may have a rather limited potential (in the range of 10%–20%) for narrowing the uncertainty of the future predictions of flood extremes. Although these results do not allow us to make confident claims about the trends in future extremes on these specific catchments, our findings point at the need for awareness of the large uncertainty that affects prediction of future extremes, highlighting the need for quantifying the uncertainty of hydrological projections, and, at the very least, acknowledge the large uncertainty surrounding the projections of extremes when only deterministic results are presented. At the same time, as pointed out by Fatichi et al. (2014), the lack of significant trends in our projections implies that infrastructure correctly designed with present-day variability in mind is likely to perform as expected in the future.

It is worth noting that the temperature-dependent patterns of high-intensity precipitation events may also change under warmer conditions. This is not explicitly considered in the models used in this study as rainfall and temperature generators are both dependent on cloud cover generation, but no physical dependence mimicking the Clausius–Clapeyron (C–C) relationship between precipitation intensity and temperature increase is built into the current structure of the AWE-GEN-2d model. This represents a limitation of the stochastically downscaled climate scenarios, because theory (i.e., the C–C relation) and confirmatory observations indicate that a warming climate is

expected to often cause a temperature-induced increase in extreme rainfall (Berg et al., 2009; Trenberth et al., 2003; among others), as well as modifying other spatial characteristics of storms (Fowler et al., 2021; Lochbihler et al., 2017, 2019; Peleg et al., 2018; Peleg, Skinner, et al., 2020; Wasko et al., 2016), which may have effects on the hydrological response of catchments (Peleg et al., 2021; Peleg, Sinclair, et al., 2020).

Given that our study sites are largely representative of the alpine region, it is likely that the results apply to most catchments in the European Alps. Catchments with high regulation of flow (for example, with hydropower dams) or with a large variation in land cover (e.g., large expanses covered with glaciers) may have different uncertainty compositions (Fatichi et al., 2014, 2015; Schirmer et al., 2021). Moreover, the proposed novel framework to partition hydrological uncertainties at high space–time resolution is not tailored to a specific case study and, thus, it is easily applicable to other regions, particularly when the interest is in characterizing either small catchment areas or complex topography in other climates beyond the European Alps. As a result, this work contributes to expanding the applicability of climate change uncertainty quantification studies.

5 | CONCLUSIONS

This article presents a novel framework for quantifying and partitioning the uncertainty of small-scale hydrological processes based on combining regional climate model outputs, a high-resolution weather generator, and a distributed hydrological model. Using two mountainous catchments in Switzerland as study sites, ensembles of gridded climate and hydrological variables were generated to represent the present and future climate under an RCP 8.5 emission scenario and multiple climate model chains and quantify the stochastic uncertainty of the projections. Using a newly introduced STNR metric, it is shown that, for the entire simulation period, the change signal for annual streamflow is weak, mostly due to high values of stochastic

uncertainty. The STNR of specific hydrological components such as liquid precipitation or snowmelt were, in contrast, higher and more dependent on climate model uncertainty, which suggests that improvements in climate models have the potential to narrow down the uncertainty on these variables. As a consequence, the largest potential for narrowing the uncertainty of mean streamflow was found during warm seasons and at higher elevations, where hydrological processes are more sensitive to temperature changes. As for extreme high flows, the results show low absolute values of STNR for all elevations explained by the dominant role of stochastic uncertainty, thus suggesting a limited potential for projecting flood extremes in the future with precision.

ACKNOWLEDGEMENTS

This research has been funded by the Swiss Federal Office for the Environment (FOEN), grant number 15.0003.PJ/Q123-0588. The authors acknowledge MeteoSwiss for providing meteorological observations, the Swiss National Centre for Climate Services (NCCS) for providing climate model simulations, and FOEN for providing hydrological observations.

DATA AVAILABILITY STATEMENT

The data and numerical models used in this study are available from the corresponding author upon reasonable request.

ORCID

Jorge Sebastián Moraga  <https://orcid.org/0000-0002-0883-9156>

Nadav Peleg  <https://orcid.org/0000-0001-6863-2934>

Peter Molnar  <https://orcid.org/0000-0001-6437-4931>

Simone Fatichi  <https://orcid.org/0000-0003-1361-6659>

REFERENCES

- Addor, N., Rössler, O., Köplin, N., Huss, M., Weingartner, R., & Seibert, J. (2014). Robust changes and sources of uncertainty in the projected hydrological regimes of Swiss catchments. *Water Resources Research*, 50(10), 7541–7562. <https://doi.org/10.1002/2014WR015549>
- Anandhi, A., Frei, A., Pierson, D. C., Schneideman, E. M., Zion, M. S., Lounsbury, D., & Matonse, A. H. (2011). Examination of change factor methodologies for climate change impact assessment. *Water Resources Research*, 47, W03501. <https://doi.org/10.1029/2010WR009104>
- Battista, G., Molnar, P., & Burlando, P. (2020). Modelling impacts of spatially variable erosion drivers on suspended sediment dynamics. *Earth Surface Dynamics*, 8(3), 619–635. <https://doi.org/10.5194/esurf-8-619-2020>
- Battista, G., Schlunegger, F., Burlando, P., & Molnar, P. (2020). Modelling localized sources of sediment in mountain catchments for provenance studies. *Earth Surface Processes and Landforms*, 45(14), 3475–3487. <https://doi.org/10.1002/esp.4979>
- Berg, P., Haerter, J. O., Thejll, P., Piani, C., Hagemann, S., & Christensen, J. H. (2009). Seasonal characteristics of the relationship between daily precipitation intensity and surface temperature. *Journal of Geophysical Research*, 114(D18), D18102. <https://doi.org/10.1029/2009JD012008>
- Bodeneignungskarte: 77.2 Digitale Bodeneignungskarte der Schweiz. <https://www.blw.admin.ch/blw/de/home/politik/datenmanagement/geografisches-informationssystem-gis/download-geodaten.html>, 2012.
- Camici, S., Brocca, L., & Moramarco, T. (2017). Accuracy versus variability of climate projections for flood assessment in Central Italy. *Climatic Change*, 141(2), 273–286. <https://doi.org/10.1007/s10584-016-1876-x>
- CH2018. (2018). *CH2018—Climate scenarios for Switzerland: Technical report*. National Centre for Climate Services.
- Chawla, I., & Mujumdar, P. P. (2018). Partitioning uncertainty in streamflow projections under nonstationary model conditions. *Advances in Water Resources*, 112, 266–282. <https://doi.org/10.1016/j.advwatres.2017.10.013>
- Chen, J., Brissette, F. P., Liu, P., & Xia, J. (2017). Using raw regional climate model outputs for quantifying climate change impacts on hydrology. *Hydrological Processes*, 31(24), 4398–4413. <https://doi.org/10.1002/hyp.11368>
- Clark, M. P., Wilby, R. L., Gutmann, E. D., Vano, J. A., Gangopadhyay, S., Wood, A. W., Fowler, H. J., Prudhomme, C., Arnold, J. R., & Brekke, L. D. (2016). Characterizing uncertainty of the hydrologic impacts of climate change. *Current Climate Change Reports*, 2(2), 55–64. <https://doi.org/10.1007/s40641-016-0034-x>
- CLC, 2012. Corine Land Cover (CLC) map 2012. <https://land.copernicus.eu/pan-european/corine-land-cover/clc-2012>.
- Deser, C., Knutti, R., Solomon, S., & Phillips, A. S. (2012). Communication of the role of natural variability in future North American climate. *Nature Climate Change*, 2(11), 775–779. <https://doi.org/10.1038/nclimate1562>
- Deser, C., Phillips, A., Bourdette, V., & Teng, H. (2012). Uncertainty in climate projections: The role of internal variability. *Climate Dynamics*, 38(3–4), 527–546. <https://doi.org/10.1007/s00382-010-0977-x>
- Deser, C. (2020). Certain uncertainty: The role of internal climate variability in projections of regional climate change and risk management. *Earth's Future*, 8(12), e2020EF001854. <https://doi.org/10.1029/2020ef001854>
- Fatichi, S., Ivanov, V. Y., & Caporali, E. (2011). Simulation of future climate scenarios with a weather generator. *Advances in Water Resources*, 34(4), 448–467. <https://doi.org/10.1016/j.advwatres.2010.12.013>
- Fatichi, S., Ivanov, V. Y., Paschalis, A., Peleg, N., Molnar, P., Rimkus, S., Kim, J., Burlando, P., & Caporali, E. (2016). Uncertainty partition challenges the predictability of vital details of climate change. *Earth's Future*, 4(5), 240–251. <https://doi.org/10.1002/2015EF000336>
- Fatichi, S., Rimkus, S., Burlando, P., Bordoy, R., & Molnar, P. (2015). High-resolution distributed analysis of climate and anthropogenic changes on the hydrology of an alpine catchment. *Journal of Hydrology*, 525, 362–382. <https://doi.org/10.1016/j.jhydrol.2015.03.036>
- Fatichi, S., Rimkus, S., Burlando, P., & Bordoy, R. (2014). Does internal climate variability overwhelm climate change signals in streamflow? The upper Po and Rhone basin case studies. *Science of the Total Environment*, 493, 1171–1182. <https://doi.org/10.1016/j.scitotenv.2013.12.014>
- Feng, D., & Beighley, E. (2020). Identifying uncertainties in hydrologic fluxes and seasonality from hydrologic model components for climate change impact assessments. *Hydrology and Earth System Sciences*, 24(5), 2253–2267. <https://doi.org/10.5194/hess-24-2253-2020>
- Fowler, H. J., Lenderink, G., Prein, A. F., Westra, S., Allan, R. P., Ban, N., Barbero, R., Berg, P., Blenkinsop, S., Do, H. X., Guerreiro S., Haerter, J. O., Kendon, E. J., Lewis, E., Schaer, C., Sharma, A., Villarini, G., Wasko, C., Zhang, X. (2021). Anthropogenic intensification of short-duration rainfall extremes. *Nature Reviews Earth & Environment*, 2(2), 107–122. <https://doi.org/10.1038/s43017-020-00128-6>
- Gao, C., & Booij, M. J. (2020). Assessment of extreme flows and uncertainty under climate change: Disentangling the uncertainty contribution of representative concentration pathways, global climate models and internal climate variability. *Hydrology and Earth System Sciences*, 24(6), 3251–3269. <https://doi.org/10.5194/hess-24-3251-2020>

- Germann, U., Galli, G., Boscacci, M., & Bolliger, M. (2006). Radar precipitation measurement in a mountainous region. *Quarterly Journal of the Royal Meteorological Society*, 132(618 A), 1669–1692. <https://doi.org/10.1256/qj.05.190>
- Giuntoli, I., Villarini, G., Prudhomme, C., & Hannah, D. M. (2018). Uncertainties in projected runoff over the conterminous United States. *Climatic Change*, 150(3–4), 149–162. <https://doi.org/10.1007/s10584-018-2280-5>
- Hawkins, E., & Sutton, R. (2009). The potential to narrow uncertainty in regional climate predictions. *Bulletin of the American Meteorological Society*, 90(8), 1095–1107. <https://doi.org/10.1175/2009BAMS2607.1>
- Hawkins, E., & Sutton, R. (2011). The potential to narrow uncertainty in projections of regional precipitation change. *Climate Dynamics*, 37(1–2), 407–418. <https://doi.org/10.1007/s00382-010-0810-6>
- Hoegh-Guldberg, O., Jacob, D., Bindi, M., Brown, S., Camilloni, I., Diedhiou, A., Djalante, R., Ebi, K., Engelbrecht, F., Guiot, J., Hijjoka, Y., Mehrotra, S., Payne, A., Seneviratne, S. I., Thomas, A., Warren, R., Zhou, G., Halim, S. A., Achlatis, M., ... Zhou, G. (2018). Chapter 3: Impacts of 1.5°C global warming on natural and human systems. In *Global warming of 1.5°C. An IPCC special report on the impacts of global warming of 1.5°C above preindustrial levels and related global greenhouse gas emission pathways* [...]. Special Report (pp. 175–311). Intergovernmental Panel on Climate Change.
- Jacob, D., Petersen, J., Eggert, B., Alias, A., Christensen, O. B., Bouwer, L. M., Braun, A., Colette, A., Déqué, M., Georgievski, G., Georgopoulou, E., Gobiet, A., Menut, L., Nikulin, G., Haensler, A., Hempelmann, N., Jones, C., Keuler, K., Kovats, S., ... Yiou, P. (2014). EURO-CORDEX: New high-resolution climate change projections for European impact research. *Regional Environmental Change*, 14(2), 563–578. <https://doi.org/10.1007/s10113-013-0499-2>
- Jenkinson, A. F. (1955). The frequency distribution of the annual maximum (or minimum) values of meteorological elements. *Quarterly Journal of the Royal Meteorological Society*, 81(348), 158–171. <https://doi.org/10.1002/QJ.49708134804>
- Kotlarski, S., Keuler, K., Christensen, O. B., Colette, A., Déqué, M., Gobiet, A., Goergen, K., Jacob, D., Lüthi, D., Van Meijgaard, E., Nikulin, G., Schär, C., Teichmann, C., Vautard, R., Warrach-Sagi, K., & Wulfmeyer, V. (2014). Regional climate modeling on European scales: A joint standard evaluation of the EURO-CORDEX RCM ensemble. *Geoscientific Model Development*, 7, 1297–1333. <https://doi.org/10.5194/gmd-7-1297-2014>
- Lehner, F., Deser, C., Maher, N., Marotzke, J., Fischer, E., Brunner, L., Knutti, R., & Hawkins, E. (2020). Partitioning climate projection uncertainty with multiple large ensembles and CMIP5/6. *Earth System Dynamics Discussions*, 11(2), 1–28. <https://doi.org/10.5194/esd-2019-93>
- Lenderink, G., Buishand, A., & Van Deursen, W. (2007). Estimates of future discharges of the river Rhine using two scenario methodologies: Direct versus delta approach. *Hydrology and Earth System Sciences*, 11(3), 1145–1159. <https://doi.org/10.5194/HESS-11-1145-2007>
- Liu, Z., & Todini, E. (2005). Assessing the TOPKAPI non-linear reservoir cascade approximation by means of a characteristic lines solution. *Hydrological Processes*, 19(10), 1983–2006. <https://doi.org/10.1002/hyp.5662>
- Lochbihler, K., Lenderink, G., & Siebesma, A. P. (2017). The spatial extent of rainfall events and its relation to precipitation scaling. *Geophysical Research Letters*, 44(16), 8629–8636. <https://doi.org/10.1002/2017GL074857>
- Lochbihler, K., Lenderink, G., & Siebesma, A. P. (2019). Response of extreme precipitating cell structures to atmospheric warming. *Journal of Geophysical Research. Atmospheres*, 124(13), 6918. <https://doi.org/10.1029/2018JD029954>
- Magilligan, F. J., & Nislow, K. H. (2005). Changes in hydrologic regime by dams. *Geomorphology*, 71(1–2), 61–78. <https://doi.org/10.1016/J.GEOMORPH.2004.08.017>
- MeteoSwiss, 2016. Daily Precipitation (Final Analysis): RhiresD, Switzerland. <http://www.meteoswiss.admin.ch/home/search.subpage.html/en/data/products/2014/raeumliche-daten-niederschlag.html>
- Minville, M., Brissette, F., & Leconte, R. (2008). Uncertainty of the impact of climate change on the hydrology of a nordic watershed. *Journal of Hydrology*, 358(1–2), 70–83. <https://doi.org/10.1016/j.jhydrol.2008.05.033>
- Moraga, J. S., Peleg, N., Fatichi, S., Molnar, P., & Burlando, P. (2021). Revealing the impacts of climate change on mountainous catchments through high-resolution modelling. *Journal of Hydrology*, 603, 126806. <https://doi.org/10.1016/j.jhydrol.2021.126806>
- Pappas, C., Fatichi, S., Rinkus, S., Burlando, P., & Huber, M. O. (2015). The role of local-scale heterogeneities in terrestrial ecosystem modeling. *Journal of Geophysical Research, Biogeosciences*, 120(2), 341–360. <https://doi.org/10.1002/2014JG002735>
- Paschalis, A., Fatichi, S., Molnar, P., Rinkus, S., & Burlando, P. (2014). On the effects of small scale space-time variability of rainfall on basin flood response. *Journal of Hydrology*, 514, 313–327. <https://doi.org/10.1016/j.jhydrol.2014.04.014>
- Peleg, N., Fatichi, S., Paschalis, A., Molnar, P., & Burlando, P. (2017). An advanced stochastic weather generator for simulating 2-D high-resolution climate variables. *Journal of Advances in Modeling Earth Systems*, 9(3), 1595–1627. <https://doi.org/10.1002/2016MS000854>
- Peleg, N., Marra, F., Fatichi, S., Molnar, P., Morin, E., Sharma, A., & Burlando, P. (2018). Intensification of convective rain cells at warmer temperatures observed from high-resolution weather radar data. *Journal of Hydrometeorology*, 19, 715–726. <https://doi.org/10.1175/JHM-D-17-0158.1>
- Peleg, N., Molnar, P., Burlando, P., & Fatichi, S. (2019). Exploring stochastic climate uncertainty in space and time using a gridded hourly weather generator. *Journal of Hydrology*, 571(3), 627–641. <https://doi.org/10.1016/j.jhydrol.2019.02.010>
- Peleg, N., Sinclair, S., Fatichi, S., & Burlando, P. (2020). Downscaling climate projections over large and data sparse regions: Methodological application in the Zambezi River basin. *International Journal of Climatology*, 40, 6242–6264. <https://doi.org/10.1002/joc.6578>
- Peleg, N., Skinner, C., Fatichi, S., & Molnar, P. (2020). Temperature effects on the spatial structure of heavy rainfall modify catchment hydro-morphological response. *Earth Surface Dynamics*, 8, 17–36. <https://doi.org/10.5194/esurf-8-17-2020>
- Peleg, N., Skinner, C., Ramirez, J. A., & Molnar, P. (2021). Rainfall spatial-heterogeneity accelerates landscape evolution processes. *Geomorphology*, 390, 107863. <https://doi.org/10.1016/J.GEOMORPH.2021.107863>
- Priestley, C. H. B., & Taylor, R. J. (1972). On the assessment of surface heat flux and evaporation using large-scale parameters. *Monthly Weather Review*, 100(2), 81–92. [https://doi.org/10.1175/1520-0493\(1972\)100<0081:otaosh>2.3.co;2](https://doi.org/10.1175/1520-0493(1972)100<0081:otaosh>2.3.co;2)
- Rasmussen, J., Sonnenborg, T. O., Stisen, S., Seaby, L. P., Christensen, B. S. B., & Hinsby, K. (2012). Climate change effects on irrigation demands and minimum stream discharge: Impact of bias-correction method. *Hydrology and Earth System Sciences*, 16(12), 4675–4691. <https://doi.org/10.5194/HESS-16-4675-2012>
- van Roosmalen, L., Sonnenborg, T. O., Jensen, K. H., & Christensen, J. H. (2011). Comparison of hydrological simulations of climate change using perturbation of observations and distribution-based scaling. *Vadose Zone Journal*, 10(1), 136–150. <https://doi.org/10.2136/VZJ2010.0112>
- Shen, M., Chen, J., Zhuan, M., Chen, H., Xu, C. Y., & Xiong, L. (2018). Estimating uncertainty and its temporal variation related to global climate models in quantifying climate change impacts on hydrology. *Journal of Hydrology*, 556, 10–24. <https://doi.org/10.1016/j.jhydrol.2017.11.004>
- Schirmer, M., Winstral, A., Jonas, T., Burlando, P., & Peleg, N. (2021). Natural climate variability is an important aspect of future projections of

- snow water resources and rain-on-snow events. *The Cryosphere Discussions*, 1–27 [in review]. <https://doi.org/10.5194/tc-2021-276>
- Swisstopo. (2002). *DHM25: Das digitale Höhenmodell der Schweiz, Level 2*. Bundesamt für Landestopographie.
- Teutschbein, C., & Seibert, J. (2012). Bias correction of regional climate model simulations for hydrological climate-change impact studies: Review and evaluation of different methods. *Journal of Hydrology*, 456–457, 12–29. <https://doi.org/10.1016/J.JHYDROL.2012.05.052>
- Thompson, D. W. J., Barnes, E. A., Deser, C., Foust, W. E., Phillips, A. S., Thompson, D. W. J., Barnes, E. A., Deser, C., Foust, W. E., & Phillips, A. S. (2015). Quantifying the role of internal climate variability in future climate trends. *Journal of Climate*, 28(16), 6443–6456. <https://doi.org/10.1175/JCLI-D-14-00830.1>
- Trenberth, K. E., Dai, A., Rasmussen, R. M., & Parsons, D. B. (2003). The changing character of precipitation. *Bulletin of the American Meteorological Society*, 84(9), 1205–1217+1161. <https://doi.org/10.1175/BAMS-84-9-1205>
- Vetter, T., Reinhardt, J., Flörke, M., van Griensven, A., Hattermann, F., Huang, S., Koch, H., Pechlivanidis, I. G., Plötner, S., Seidou, O., Su, B., Vervoort, R. W., & Krysanova, V. (2017). Evaluation of sources of uncertainty in projected hydrological changes under climate change in 12 large-scale river basins. *Climatic Change*, 141(3), 419–433. <https://doi.org/10.1007/s10584-016-1794-y>
- Wasko, C., Sharma, A., & Westra, S. (2016). Reduced spatial extent of extreme storms at higher temperatures. *Geophysical Research Letters*, 43(8), 4026–4032. <https://doi.org/10.1002/2016GL068509>
- Wüest, M., Frei, C., Altenhoff, A., Hagen, M., Litschi, M., & Schär, C. (2009). A gridded hourly precipitation dataset for Switzerland using rain-gauge analysis and radar-based disaggregation. *International Journal of Climatology*, 30(12), 1775. <https://doi.org/10.1002/joc.2025>

SUPPORTING INFORMATION

Additional supporting information can be found online in the Supporting Information section at the end of this article.

How to cite this article: Moraga, J. S., Peleg, N., Molnar, P., Fatichi, S., & Burlando, P. (2022). Uncertainty in high-resolution hydrological projections: Partitioning the influence of climate models and natural climate variability. *Hydrological Processes*, 36(10), e14695. <https://doi.org/10.1002/hyp.14695>